

Mueller Navelet jets at LHC: A clean test of QCD resummation effects at high energy?

Bertrand Ducloué

Laboratoire de Physique Théorique
Orsay, France

2nd Workshop on QCD and Diffraction at the LHC

Cracow, November 27th 2012

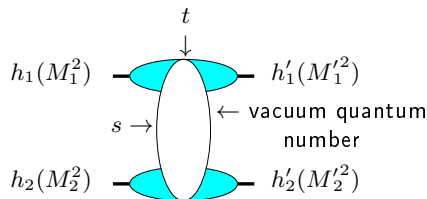
in collaboration with

L. Szymanowski (NCBJ, Warsaw), S. Wallon (UPMC & LPT Orsay)

D. Colferai; F. Schwennsen, L. Szymanowski, S. Wallon
JHEP 1012:026 (2010) 1-72 [arXiv:1002.1365 [hep-ph]]

B.D., L. Szymanowski, S. Wallon, in preparation

- One of the important longstanding theoretical questions raised by QCD is its behaviour in the perturbative **Regge** limit $s \gg -t$
- Based on theoretical grounds, one should identify and test suitable observables in order to test this peculiar dynamics



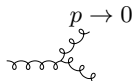
hard scales: $M_1^2, M_2^2 \gg \Lambda_{QCD}^2$ or $M_1'^2, M_2'^2 \gg \Lambda_{QCD}^2$ or $t \gg \Lambda_{QCD}^2$
 where the t -channel exchanged state is the so-called **hard Pomeron**

What kind of observables?

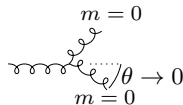
- perturbation theory should be applicable:

selecting external or internal probes with transverse sizes $\ll 1/\Lambda_{QCD}$ or by choosing large t in order to provide the hard scale

- governed by the "soft" perturbative dynamics of QCD



and *not* by its collinear dynamics



\Rightarrow select semi-hard processes with $s \gg p_{T,i}^2 \gg \Lambda_{QCD}^2$ where $p_{T,i}^2$ are typical transverse scale, all of the same order

Some examples of processes

- **inclusive:** DIS (HERA), diffractive DIS, total $\gamma^*\gamma^*$ cross-section (LEP, ILC)
- **semi-inclusive:** forward jet and π^0 production in DIS, Mueller-Navelet double jets, diffractive double jets, high p_T central jet, in hadron-hadron colliders (Tevatron, LHC)
- **exclusive:** exclusive meson production in DIS, double diffractive meson production at e^+e^- colliders (ILC), ultraperipheral events at LHC (Pomeron, Odderon)

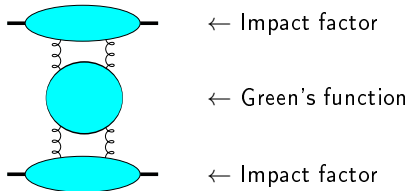
QCD in the perturbative Regge limit

- Small values of α_s (perturbation theory applies due to hard scales) can be compensated by large $\ln s$ enhancements.
 \Rightarrow resummation of $\sum_n (\alpha_s \ln s)^n$ series (Balitski, Fadin, Kuraev, Lipatov)
 \rightarrow introduction of a new arbitrary scale s_0 : $\ln s \rightarrow \ln \frac{s}{s_0}$

$$\mathcal{A} = \underbrace{\text{Diagram 1}}_{\sim s} + \left(\text{Diagram 2} + \text{Diagram 3} + \dots \right)_{\sim s (\alpha_s \ln s)} + \left(\text{Diagram 4} + \dots \right)_{\sim s (\alpha_s \ln s)^2} + \dots$$

The diagrams represent different orders of perturbation theory. Diagram 1 is a tree-level exchange. Diagrams 2 and 3 show one-loop corrections with different topologies. Diagram 4 shows a two-loop correction. The ellipses indicate higher-order terms in the series.

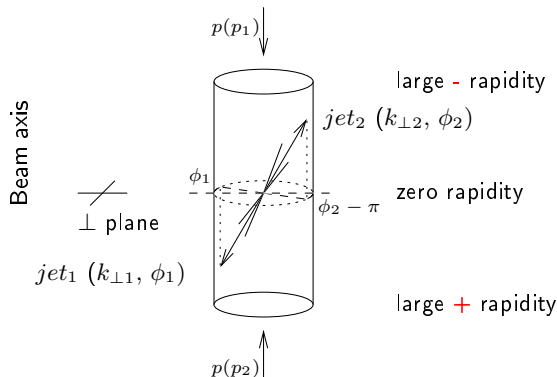
- this can be put in the following form :



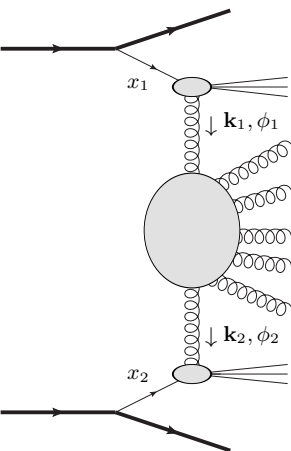
- Higher order corrections to BFKL kernel are known at NLL order (Lipatov Fadin; Camici, Ciafaloni), now for arbitrary impact parameter $\alpha_S \sum_n (\alpha_S \ln s)^n$ resummation
- impact factors are known in some cases at NLL
 - $\gamma^* \rightarrow \gamma^*$ at $t = 0$ (Bartels, Colferai, Gieseke, Kyrieleis, Qiao; Balitski, Chirilli)
 - forward jet production (Bartels, Colferai, Vacca)
 - inclusive production of a pair of hadrons separated by a large interval of rapidity (Ivanov, Papa)
 - $\gamma_L^* \rightarrow \rho_L$ in the forward limit (Ivanov, Kotsky, Papa)

Mueller-Navelet jets

- Consider two jets (hadrons flying within a narrow cone) **separated by a large rapidity**, i.e. each of them almost fly in the direction of the hadron “close” to it, and with very similar transverse momenta
- in a pure LO collinear treatment, these two jets should be emitted **back to back** at leading order: $\Delta\phi - \pi = 0$ ($\Delta\phi = \phi_1 - \phi_2 =$ relative azimuthal angle) and $k_{\perp 1} = k_{\perp 2}$. There is no phase space for (untagged) emission between them



k_T -factorized differential cross-section



$$\frac{d\sigma}{d|\mathbf{k}_{J1}| d|\mathbf{k}_{J2}| dy_{J1} dy_{J2}} = \int d\phi_{J1} d\phi_{J2} \int d^2\mathbf{k}_1 d^2\mathbf{k}_2$$

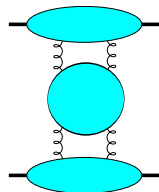
$$\times \Phi(\mathbf{k}_{J1}, x_{J1}, -\mathbf{k}_1)$$

$$\times G(\mathbf{k}_1, \mathbf{k}_2, \hat{s})$$

$$\times \Phi(\mathbf{k}_{J2}, x_{J2}, \mathbf{k}_2)$$

with $\Phi(\mathbf{k}_{J2}, x_{J2}, \mathbf{k}_2) = \int dx_2 f(x_2) V(\mathbf{k}_2, x_2)$ $f \equiv \text{PDF}$ $x_J = \frac{|\mathbf{k}_J|}{\sqrt{s}} e^{y_J}$

- in **LL BFKL** ($\sim \sum (\alpha_s \ln s)^n$), the emission between these jets leads to a **strong decorrelation** between the jets, incompatible with $p\bar{p}$ **Tevatron** collider data
- up to recently, the subseries $\alpha_s \sum (\alpha_s \ln s)^n$ **NLL** was included only in the Green's function, and not inside the jet vertices
Sabio Vera, Schwennsen
Marquet, Royon
- the importance of these corrections was not known



Because of the structure of the NLL jet vertex, numerical implementation is quite delicate (requires special grouping of the terms, etc.)

- First study done with a Mathematica code
rather slow \Rightarrow access to a limited number of configurations

D. Colferai; F. Schwennsen, L. Szymanowski, S. Wallon
JHEP 1012:026 (2010) 1-72

- New Fortran code
 - much faster
 - Check of the Mathematica based results
 - Stability studies (PDFs, etc.) made easier
 - Check of previous mixed studies (NLL Green's function + LL jet vertices)
 - Allows for k_J integration over a finite range
 - A comparison with the recent small R study of D. Yu. Ivanov et al. has been performed
 - Study of the azimuthal distribution
 - More detailed comparison with NLO DGLAP
 - Problems remain with ν integration for low Y (<4)

B.D., L. Szymanowski, S. Wallon., in preparation

In practice

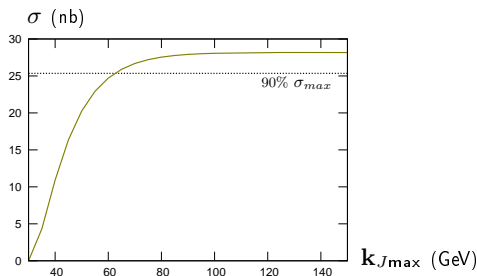
Following results are with:

- $\sqrt{s} = 7 \text{ TeV}$
- jet cone-algorithm with $R = 0.5$
- MSTW 2008 PDFs
- $\mu_R = \mu_F = \mu$ (imposed by the PDFs)
- μ and $\sqrt{s_0}$ set equal to $\sqrt{k_{J1}k_{J2}}$
- two-loop running coupling $\alpha_s(\mu^2)$ with $\alpha_s(M_Z^2) = 0.1176$

Previous results ([arxiv:1002.1365](https://arxiv.org/abs/1002.1365)) were shown for fixed $|\mathbf{k}_{J1}|$ and $|\mathbf{k}_{J2}|$. But experimental data is integrated over some range, $\mathbf{k}_{J\min} \leq |\mathbf{k}_{J1}|, |\mathbf{k}_{J2}|$

With our faster code we are now able to integrate $|\mathbf{k}_{J1}|$ and $|\mathbf{k}_{J2}|$ over some finite range

Because the cross section decreases quickly with the transverse momentum of jets, we can choose an upper bound for $|\mathbf{k}_{J1,2}|$ to get a good estimate of the total cross section.



\Rightarrow for $\mathbf{k}_{J\min} = 35$ GeV, we need to integrate up to $\mathbf{k}_{J\max} \sim 60$ GeV

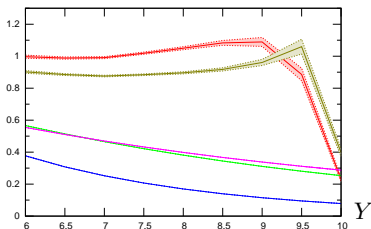
Energy-momentum conservation issues

- BFKL does not preserve energy-momentum conservation
- This violation is expected to be smaller at higher order in perturbation theory, i.e. NLL versus LL
- In practice: avoid to use all the available collider energy:
 $y_{J,i} \ll \cosh^{-1} \frac{x_i E}{|\mathbf{k}_{J,i}|}$
 \rightarrow A lower $|\mathbf{k}_J|$ means a larger validity domain : a $|\mathbf{k}_J|$ as small as possible is preferable
- With only a lower cut on $|\mathbf{k}_J|$, one has to integrate over regions where the BFKL approach may not be valid anymore : $|\mathbf{k}_J| = 60 \text{ GeV} \rightarrow Y \ll 7.3$
- For this reason it would be nice to have a measurement with also an upper cut on transverse momentum, $\mathbf{k}_{J\min} \leq \mathbf{k}_J \leq \mathbf{k}_{J\max}$

Azimuthal correlation $\langle \cos \varphi \rangle$: more on the (anti)collinear resummation effects

In the previous study the collinear resummation (Salam; Ciafaloni, Colferai) was only taken into account for $n = 0$

$$\frac{C_1}{C_0} = \langle \cos \varphi \rangle$$



pure LL

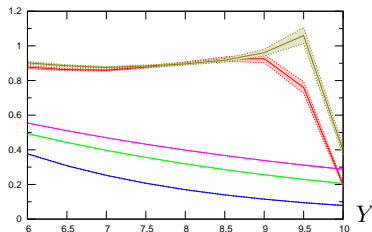
LL vertices + NLL Green's fun.

LL vertices + NLL resum. ($n = 0$) Green's fun.

NLL vertices + NLL Green's fun.

NLL vertices + NLL resum. ($n = 0$) Green's fun.

$$\frac{C_1}{C_0} = \langle \cos \varphi \rangle$$



pure LL

LL vertices + NLL Green's fun.

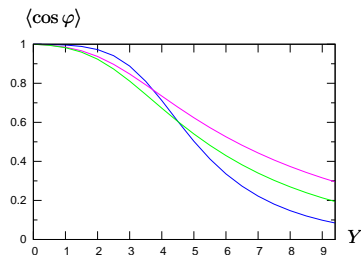
LL vertices + NLL resum. (all n) Green's fun.

NLL vertices + NLL Green's fun.

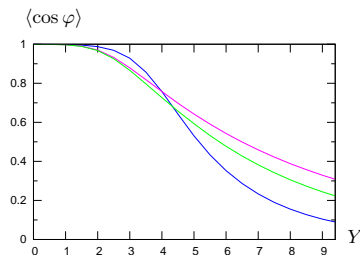
NLL vertices + NLL resum. (all n) Green's fun.

Taking into account the collinear improvement also for $n > 0$ we find the results don't change very much when using the NLL vertex

Azimuthal correlation $\langle \cos \varphi \rangle$: more on the (anti)collinear resummation effects



Marquet, Royon



our Fortran code

pure LL

LL vertices + NLL Green's fun.

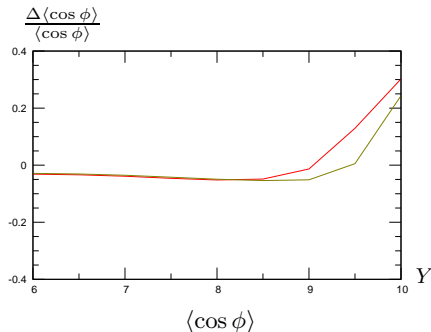
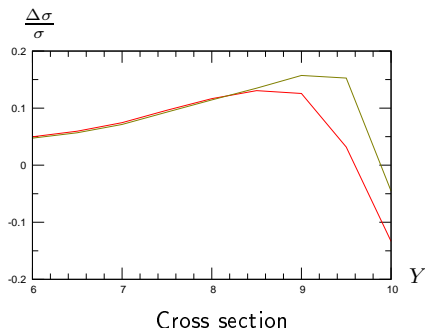
LL vertices + NLL resummed Green's fun.

Taking into account the collinear improvement also for $n > 0$ we find results close to the previous studies

Recently a computation of the jet vertex at NLO in the small cone approximation ($R \ll 1$) was made.

F. Caporale, D. Yu. Ivanov, B. Murdaca, A. Papa, A. Perri

arXiv:1112.3752 [hep-ph]

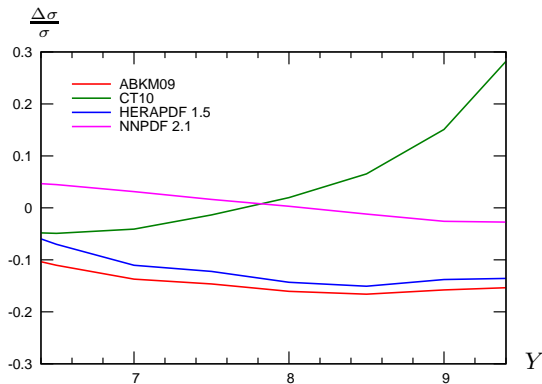


The comparison between the exact and approximate treatments shows good agreement even for a cone parameter $R = 0.5$

Note: $Y \ll 8$ for BFKL validity (e-m conservation issues)

Cross-section: PDF errors

Relative variation of the cross section when using other PDF sets than MSTW 2008 (full NLL approach)



(very similar values for the LL computation)

$\langle \cos \varphi \rangle$, $\langle \cos 2\varphi \rangle$, etc. vary by less than 2% when changing PDF set.

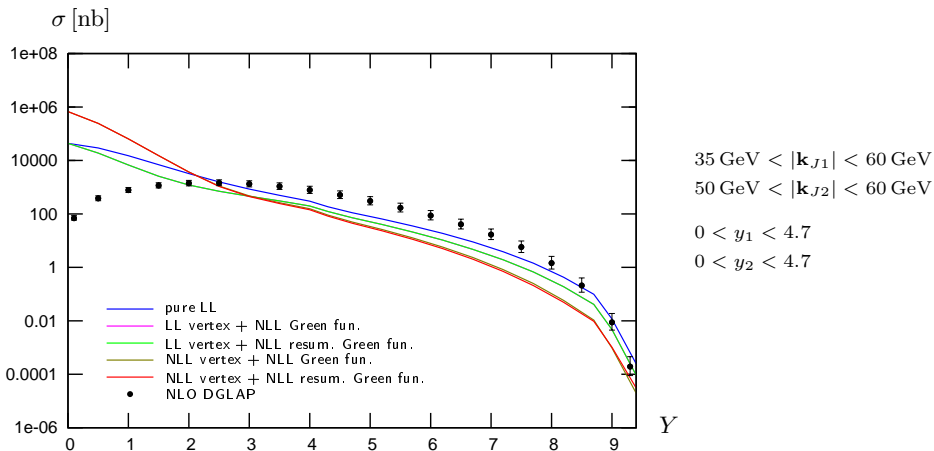
Results for an asymmetric configuration

In this section we choose the cuts as

- $35 \text{ GeV} < |\mathbf{k}_{J1}| < 60 \text{ GeV}$
- $50 \text{ GeV} < |\mathbf{k}_{J2}| < 60 \text{ GeV}$
- $0 < y_1, y_2 < 4.7$

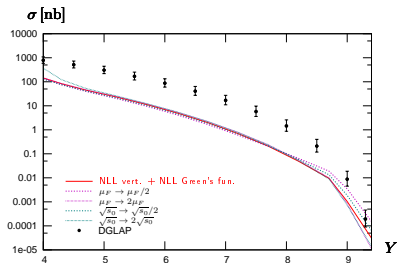
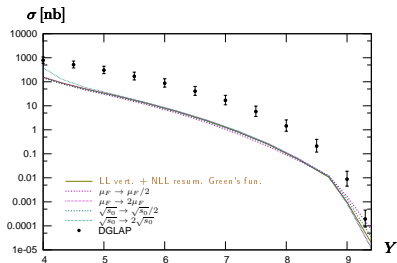
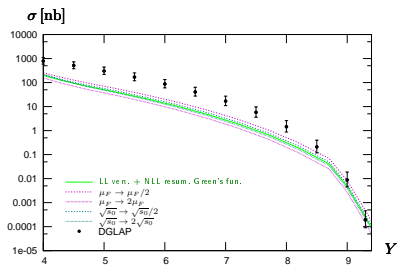
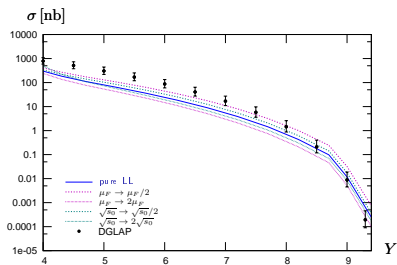
Such an asymmetric configuration is required by [DGLAP](#) like approaches, which are unstable for symmetric configurations.

Cross-section: NLO DGLAP versus NLL BFKL

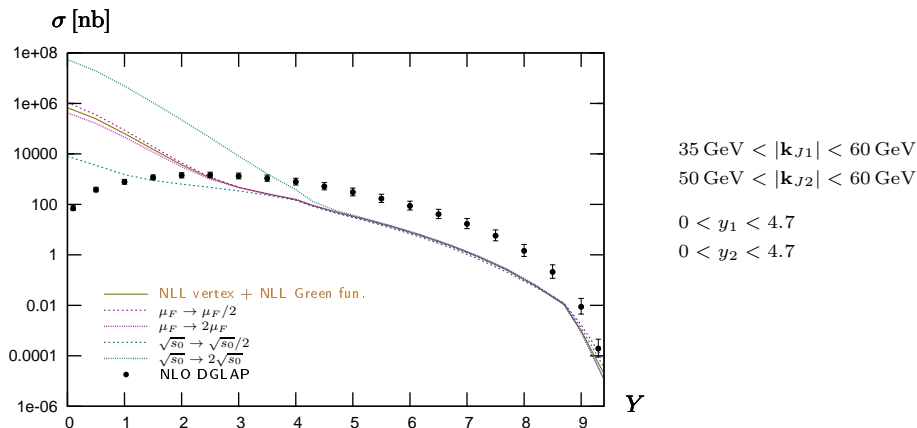


dots = based on the NLO DGLAP parton generator *Dijet* (thanks to M. Fontannaz)

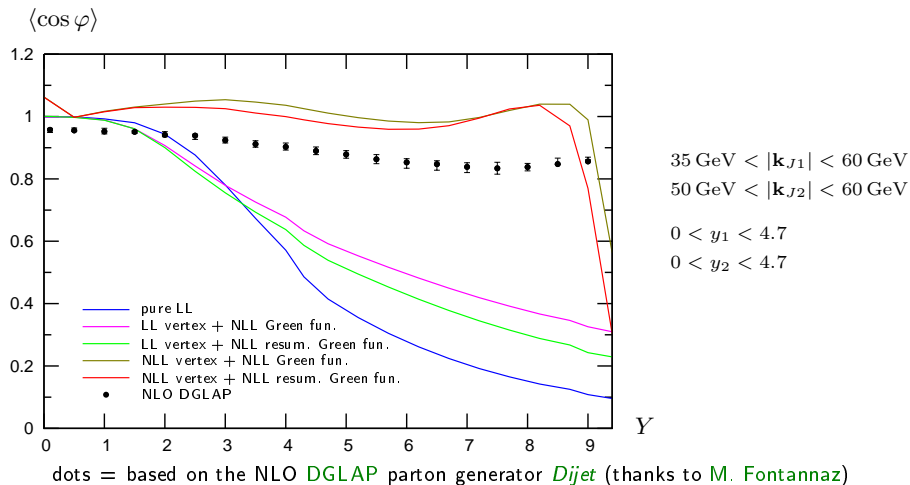
Cross-section: stability with respect to s_0 and $\mu_R = \mu_F$ changes

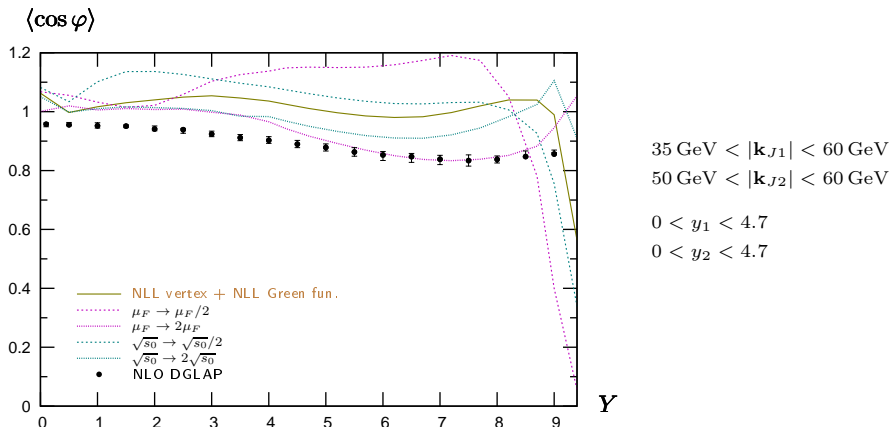


Compared cross-sections including uncertainties



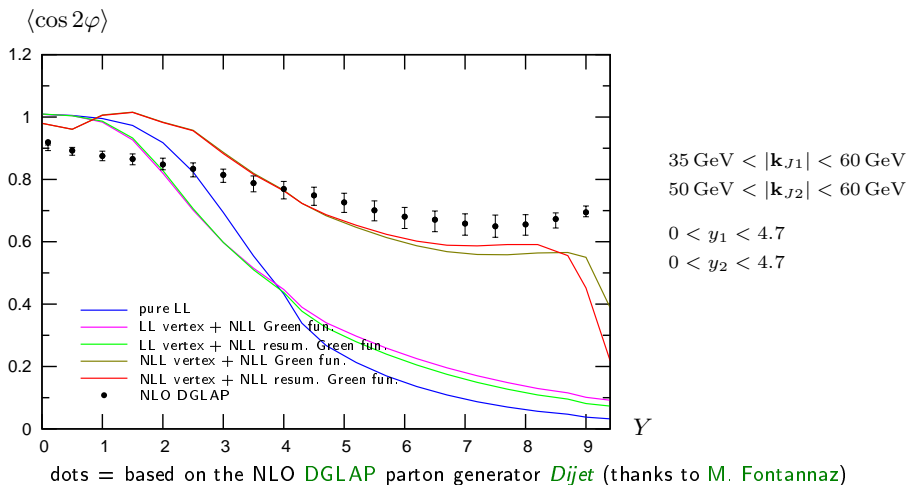
- Putting (almost) the same scale, exactly the same cuts, we get a noticeable difference between NLO DGLAP and NLL BFKL for $4.5 < Y < 8.5$: $\sigma_{\text{NLO}} > \sigma_{\text{NLL BFKL}}$
- This result is rather stable w.r.t s_0 and μ choices.

Azimuthal correlation $\langle \cos \varphi \rangle$: NLO DGLAP versus NLL BFKL

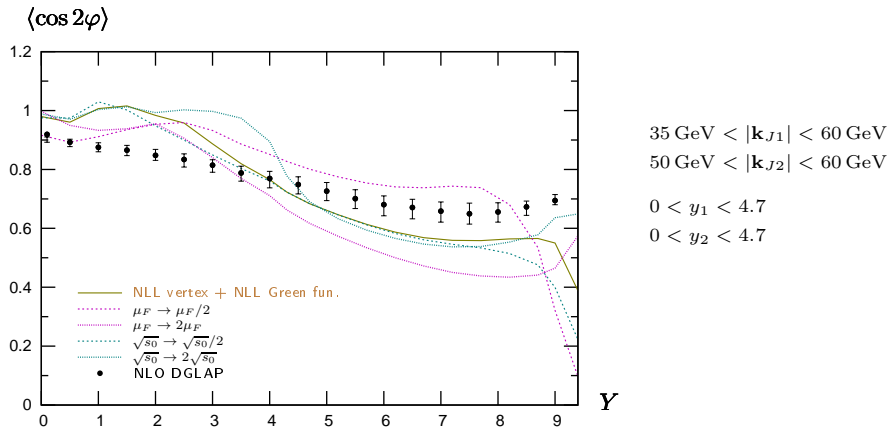
Azimuthal correlation: $\langle \cos \varphi \rangle$ 

- Putting (almost) the same scale, exactly the same cuts, we get a difference between **NLO DGLAP** and **NLL BFKL** for $4.5 < Y < 8.5$
- This difference is washed-out because of s_0 and μ dependency:

$$\langle \cos \varphi \rangle_{\text{NLO}} \sim \langle \cos \varphi \rangle_{\text{NLL BFKL}}$$

Azimuthal correlation $\langle \cos 2\varphi \rangle$: NLO versus NLL BFKL

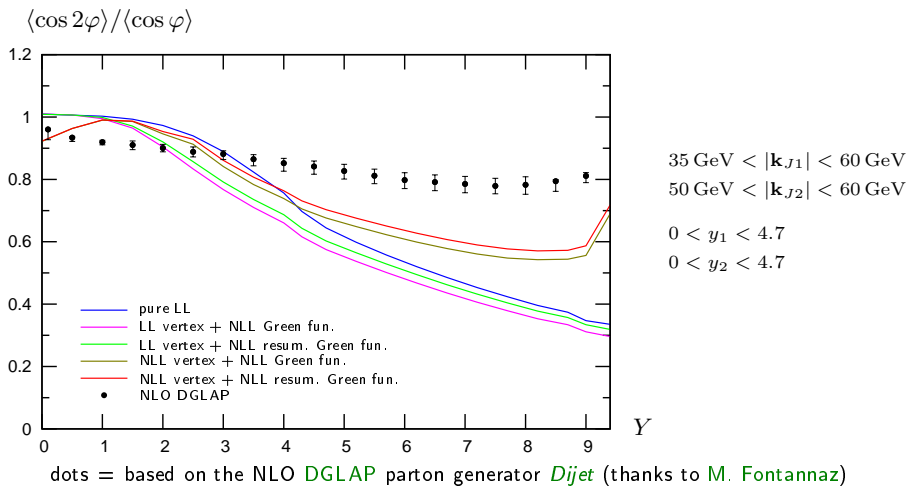
Azimuthal correlation: $\langle \cos 2\varphi \rangle$



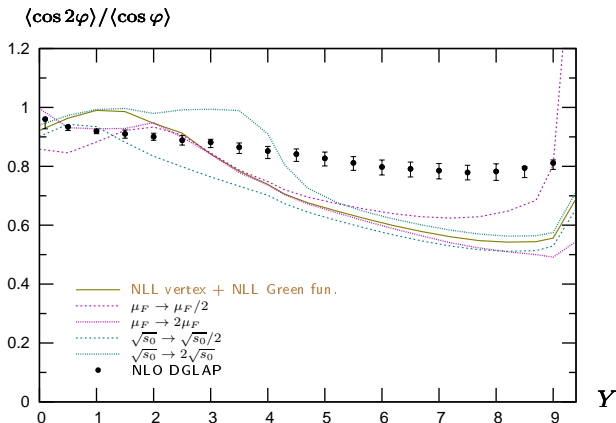
- Putting (almost) the same scale, exactly the same cuts, we get a difference between **NLO DGLAP** and **NLL BFKL** for $4.5 < Y < 8.5$
- This difference is washed-out because of s_0 and μ dependency:

$$\langle \cos 2\varphi \rangle_{\text{NLO}} \sim \langle \cos 2\varphi \rangle_{\text{NLL BFKL}}$$

Azimuthal correlation $\langle \cos 2\varphi \rangle / \langle \cos \varphi \rangle$: NLO versus NLL BFKL



Azimuthal correlation: $\langle \cos 2\varphi \rangle / \langle \cos \varphi \rangle$



$35 \text{ GeV} < |\mathbf{k}_{J1}| < 60 \text{ GeV}$

$50 \text{ GeV} < |\mathbf{k}_{J2}| < 60 \text{ GeV}$

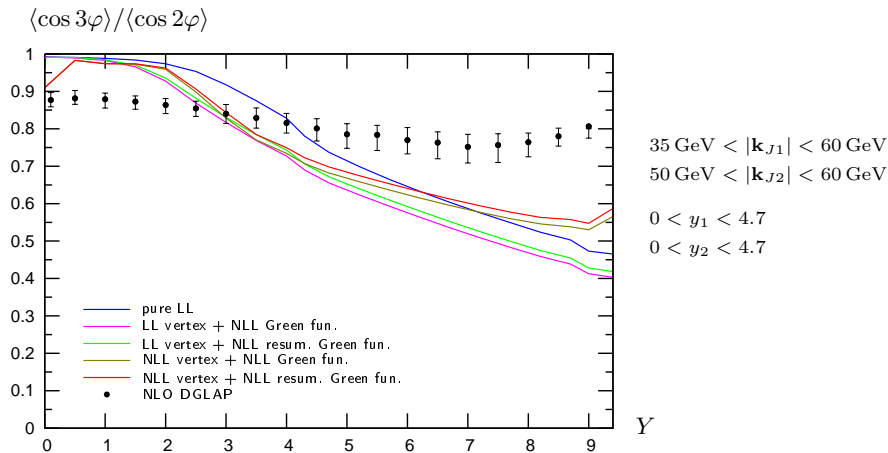
$0 < y_1 < 4.7$

$0 < y_2 < 4.7$

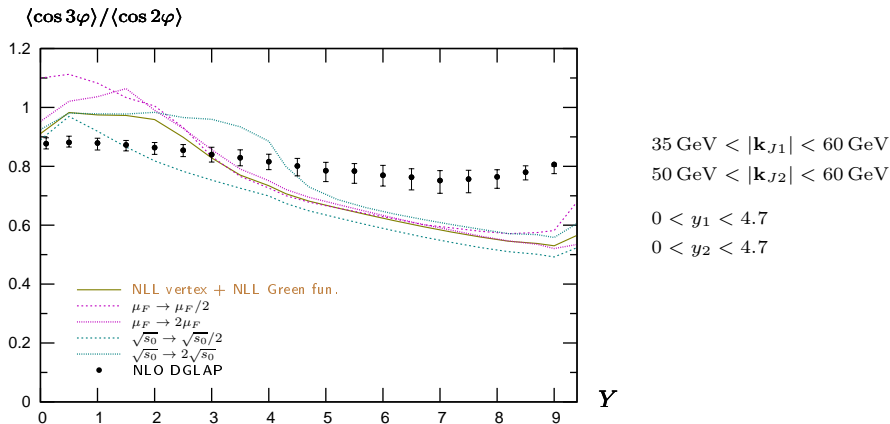
- NLO DGLAP and NLL BFKL differ for $4.5 < Y < 8$

$$\frac{\langle \cos 2\varphi \rangle_{\text{NLO}}}{\langle \cos \varphi \rangle_{\text{NLO}}} > \frac{\langle \cos 2\varphi \rangle_{\text{NLL BFKL}}}{\langle \cos \varphi \rangle_{\text{NLL BFKL}}}$$

- This result is rather stable w.r.t s_0 and μ choices.

Azimuthal correlation $\langle \cos 3\varphi \rangle / \langle \cos 2\varphi \rangle$: NLO versus NLL BFKL

dots = based on the NLO **DGLAP** parton generator *Dijet* (thanks to M. Fontannaz)

Azimuthal correlation: $\langle \cos 3\varphi \rangle / \langle \cos 2\varphi \rangle$ 

- NLO DGLAP and NLL BFKL differ for $5.5 < Y < 8.5$

$$\frac{\langle \cos 3\varphi \rangle_{\text{NLO}}}{\langle \cos 2\varphi \rangle_{\text{NLO}}} > \frac{\langle \cos 3\varphi \rangle_{\text{NLL BFKL}}}{\langle \cos 2\varphi \rangle_{\text{NLL BFKL}}}$$

- This result is rather stable w.r.t s_0 and μ choices.

Results for a symmetric configuration

In this section we show results for

- $35 \text{ GeV} < |\mathbf{k}_{J1}|, |\mathbf{k}_{J2}| < 60 \text{ GeV}$
- $0 < y_1, y_2 < 4.7$

These cuts should be close to the ones that will be used in forthcoming analyses by ATLAS or CMS.

note:

- results for $\langle \cos(n\phi) \rangle$ are similar to the asymmetric configuration
- the cross section is even larger

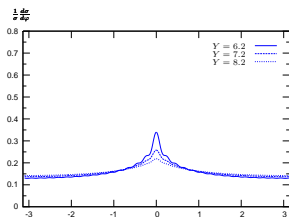
Azimuthal distribution

Computing $\langle \cos(n\phi) \rangle$ up to large values of n gives access to the angular distribution

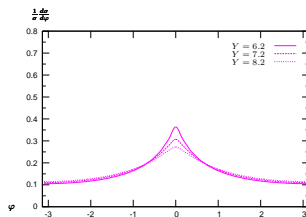
$$\frac{1}{\sigma} \frac{d\sigma}{d\phi} = \frac{1}{2\pi} \left\{ 1 + 2 \sum_{n=1}^{\infty} \cos(n\phi) \langle \cos(n\phi) \rangle \right\}$$

This is a quantity accessible at experiments like **ATLAS** and **CMS**

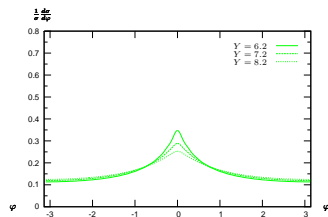
Azimuthal distribution



pure LL



LL vertices + NLL Green's fun.



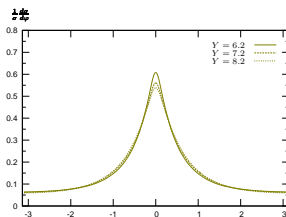
LL vert. + NLL resum. Green's fun.

$$35 \text{ GeV} < |\mathbf{k}_{J1}| < 60 \text{ GeV}$$

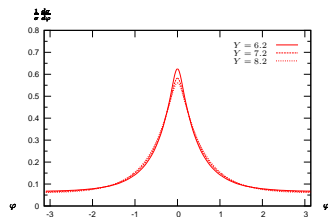
$$35 \text{ GeV} < |\mathbf{k}_{J2}| < 60 \text{ GeV}$$

$$0 < y_1 < 4.7$$

$$0 < y_2 < 4.7$$



NLL vert. + NLL Green's fun.

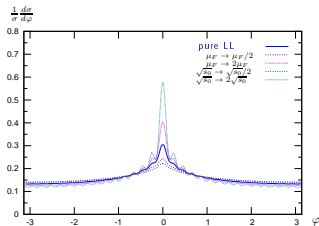


NLL vert. + NLL resum. Green's fun.

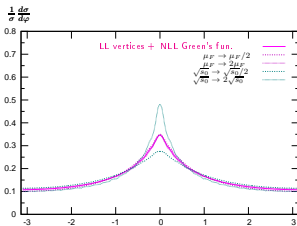
Full NLL treatment predicts :

- Less decorrelation for same Y
- Slower decorrelation with increasing Y

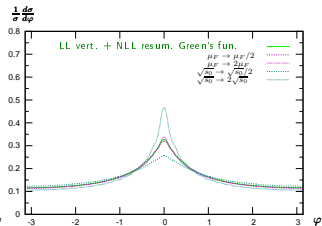
Azimuthal distribution: stability with respect to s_0 and $\mu_R = \mu_F$



pure LL



LL vertices + NLL Green's fun.



LL vert. + NLL resum. Green's fun.

$35 \text{ GeV} < |\mathbf{k}_{J1}| < 60 \text{ GeV}$

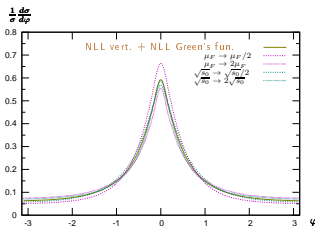
$35 \text{ GeV} < |\mathbf{k}_{J2}| < 60 \text{ GeV}$

$0 < y_1 < 4.7$

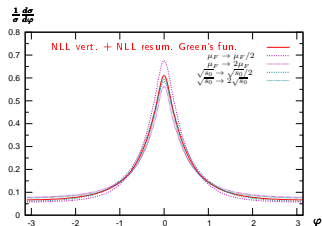
$0 < y_2 < 4.7$

integrating on the bin:

$6 < Y = y_1 + y_2 < 9.4$



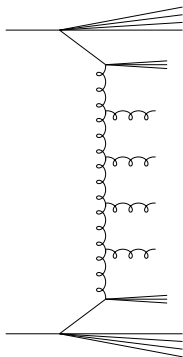
NLL vert. + NLL Green's fun.



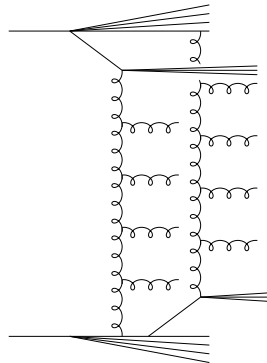
NLL vert. + NLL resum. Green's fun.

The predicted ϕ distribution within full NLL treatment is stable

Can Mueller-Navelet jets be a manifestation of multiparton interactions?

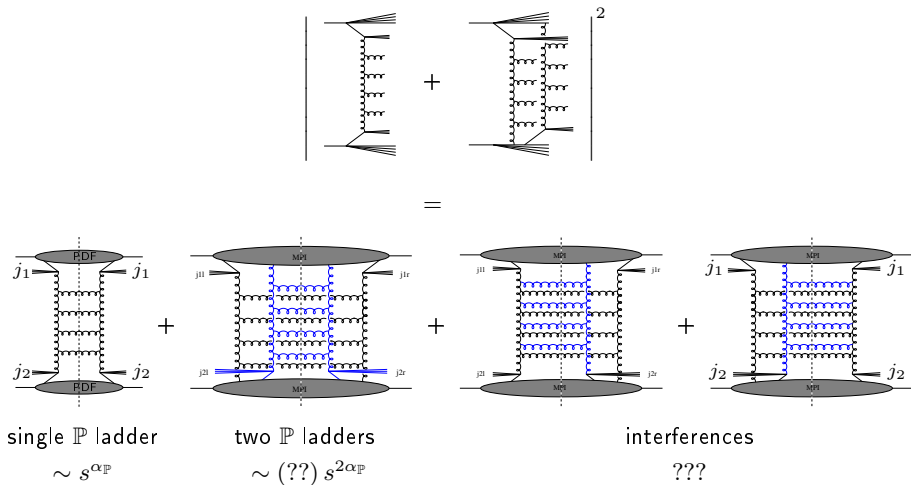


+



MN jets in the single partonic model

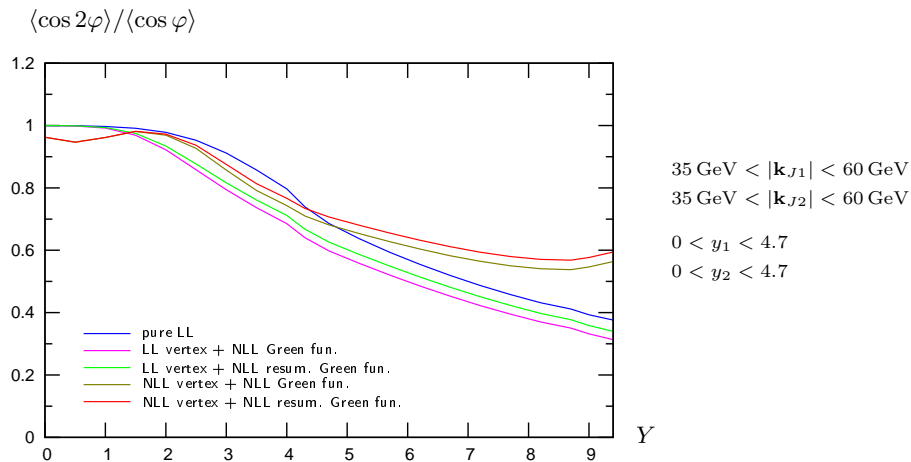
MN jets in MPI



- We have deepened our complete NLL analysis of Mueller-Navelet jets
- The effect of NLL corrections to the vertices is dramatic, similar to the NLL Green function corrections
- For the cross-section:
makes prediction more stable with respect to variation of scales μ and s_0
sizeably below NLO DGLAP
- Surprisingly small decorrelation effect
 $\langle \cos \varphi \rangle$ very flat in rapidity Y
close to NLO DGLAP when taking into account the scale dependency
- For $\langle \cos 2\varphi \rangle / \langle \cos \varphi \rangle$ and $\langle \cos 3\varphi \rangle / \langle \cos 2\varphi \rangle$ we see a difference between NLL BFKL and NLO DGLAP
- The φ distribution is strongly peaked around 0 and varies slowly with Y
- Energy-momentum conservation and MPI processes could modify the picture
- Mueller Navelet jets provide much more complicate observables than expected

Backup

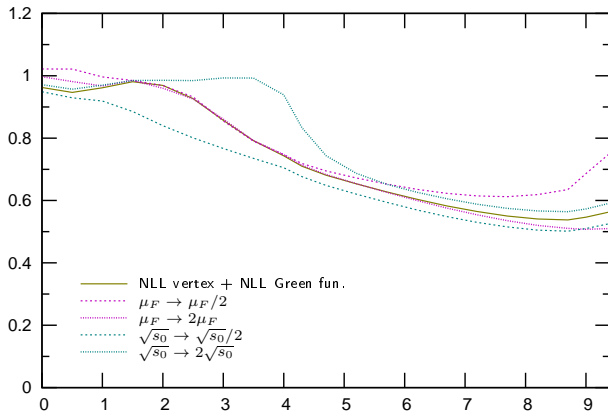
Azimuthal correlation



Azimuthal correlation: stability with respect to s_0 and $\mu_R = \mu_F$

(here only the full NLL approach is shown)

$$\langle \cos 2\varphi \rangle / \langle \cos \varphi \rangle$$



$$35 \text{ GeV} < |\mathbf{k}_{J1}| < 60 \text{ GeV}$$

$$35 \text{ GeV} < |\mathbf{k}_{J2}| < 60 \text{ GeV}$$

$$0 < y_1 < 4.7$$

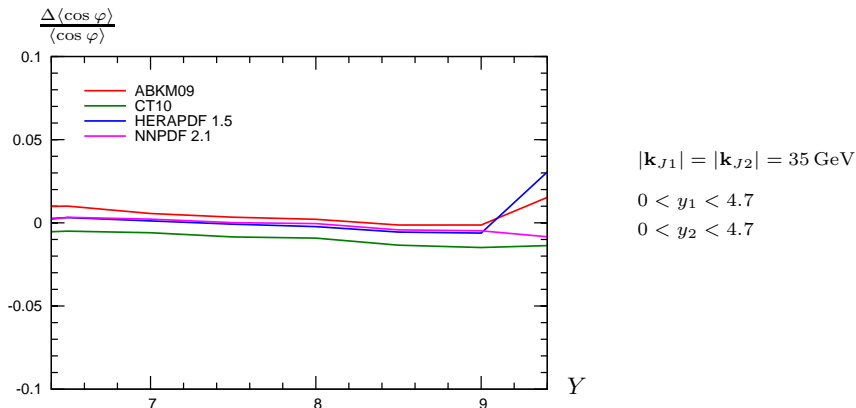
$$0 < y_2 < 4.7$$

Y

Very good stability in the range $5 < Y < 8$

Azimuthal correlation $\langle \cos \varphi \rangle$: PDF errors

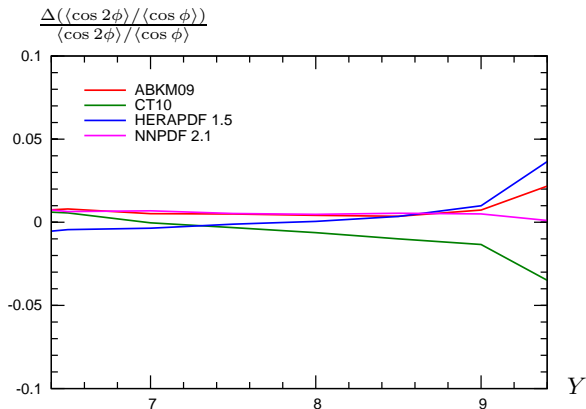
Relative variation of $\langle \cos \varphi \rangle$ when using other PDF sets than MSTW 2008 (full NLL approach)



$\langle \cos \varphi \rangle$ is much less sensitive to the PDFs than the cross section
(at LL $\langle \cos \varphi \rangle$ does not depend on the PDFs at all)

Azimuthal correlation: PDF errors

Relative variation of $\frac{\langle \cos 2\phi \rangle}{\langle \cos \phi \rangle}$ when using other PDF sets than MSTW 2008
(full NLL approach)



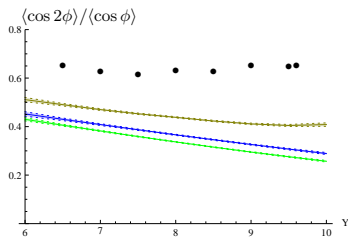
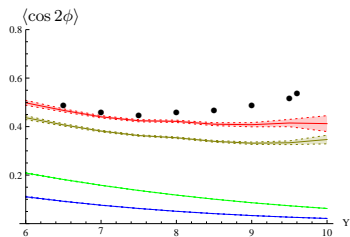
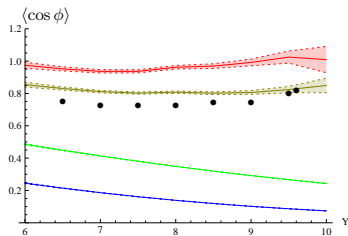
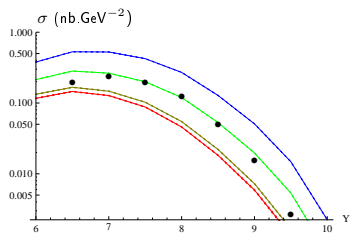
$$|\mathbf{k}_{J1}| = |\mathbf{k}_{J2}| = 35 \text{ GeV}$$

$$0 < y_1 < 4.7$$

$$0 < y_2 < 4.7$$

$\langle \cos 2\phi \rangle / \langle \cos \phi \rangle$ is much less sensitive to the PDFs than the cross section

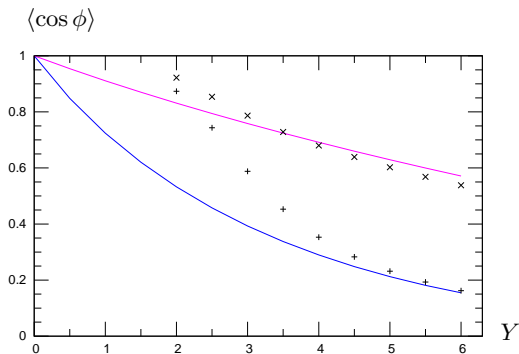
Comparison with NLO DGLAP for $\sqrt{s} = 14$ TeV



dots: based on the NLO **DGLAP** parton generator Dijet (thanks to **M. Fontannaz**)

Comparison in the simplified NLL Green's function + LL jet vertices scenario

- The integration $\int_{k_{J \min}}^{\infty} dk_J$ can be performed analytically
- A comparison with the numerical integration based on code provides a good test of stability, valid for large Y



blue: LL

magenta: NLL Green's function + LL jet vertices scenario Sabio Vera, Schwennsen

\times : numerical dk_J integration

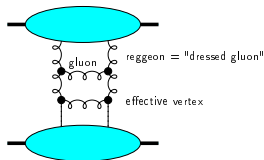
$k_{J1} > 20 \text{ GeV}$ and $k_{J2} > 50 \text{ GeV}$

QCD in the perturbative Regge limit

- Small values of α_s (perturbation theory applies due to hard scales) can be compensated by large $\ln s$ enhancements. \Rightarrow resummation of $\sum_n (\alpha_s \ln s)^n$ series (Balitski, Fadin, Kuraev, Lipatov)

$$\mathcal{A} = \underbrace{\text{Diagram 1}}_{\sim s} + \left(\underbrace{\text{Diagram 2}}_{\sim s (\alpha_s \ln s)} + \underbrace{\text{Diagram 3}}_{\sim s (\alpha_s \ln s)} + \dots \right) + \left(\underbrace{\text{Diagram 4}}_{\sim s (\alpha_s \ln s)^2} + \dots \right) + \dots$$

- this results in the effective BFKL ladder

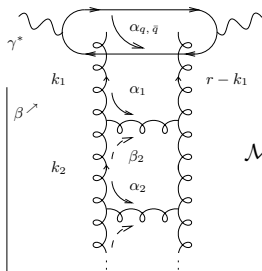


$$\Rightarrow \sigma_{tot}^{h_1 h_2 \rightarrow anything} = \frac{1}{s} \text{Im} \mathcal{A} \sim s^{\alpha_{\mathbb{P}}(0)-1}$$

with $\alpha_{\mathbb{P}}(0) - 1 = C \alpha_s$ ($C > 0$) Leading Log Pomeron
Balitsky, Fadin, Kuraev, Lipatov

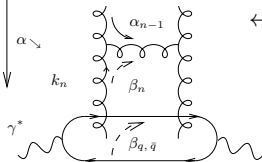
Opening the boxes: Impact representation $\gamma^* \gamma^* \rightarrow \gamma^* \gamma^*$ as an example

- Sudakov decomposition: $k_i = \alpha_i p_1 + \beta_i p_2 + k_{\perp i}$ ($p_1^2 = p_2^2 = 0$, $2p_1 \cdot p_2 = s$)
- write $d^4 k_i = \frac{s}{2} d\alpha_i d\beta_i d^2 k_{\perp i}$ ($\underline{k} = \text{Eucl.} \leftrightarrow k_{\perp} = \text{Mink.}$)
- t -channel gluons have non-sense polarizations at large s : $\epsilon_{NS}^{up/down} = \frac{2}{s} p_{2/1}$



\Rightarrow set $\alpha_1 = 0$ and $\int d\beta_1 \Rightarrow \Phi^{\gamma^* \rightarrow \gamma^*}(\underline{k}_1, \underline{r} - \underline{k}_1)$
impact factor

$$\mathcal{M} = \frac{is}{(2\pi)^2} \int \frac{d^2 \underline{k}}{\underline{k}^2} \Phi^{up}(\underline{k}, \underline{r} - \underline{k}) \int \frac{d^2 \underline{k}'}{\underline{k}'^2} \Phi^{down}(-\underline{k}', -\underline{r} + \underline{k}') \\ \times \int_{\delta-i\infty}^{\delta+i\infty} \frac{d\omega}{2\pi i} \left(\frac{s}{s_0} \right)^\omega G_\omega(\underline{k}, \underline{k}', \underline{r})$$

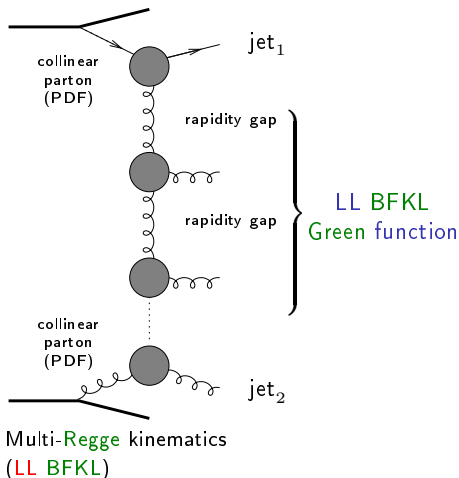


\leftarrow multi-Regge kinematics

\Rightarrow set $\beta_n = 0$ and $\int d\alpha_n \Rightarrow \Phi^{\gamma^* \rightarrow \gamma^*}(-\underline{k}_n, -\underline{r} + \underline{k}_n)$

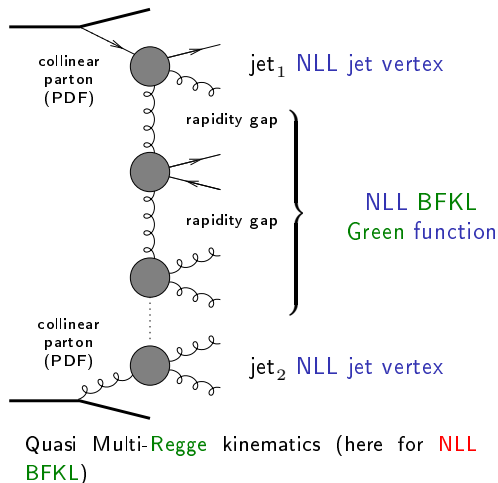
Mueller Navelet jets at LL BFKL

- in LL BFKL ($\sim \sum (\alpha_s \ln s)^n$), emission between these jets
→ **strong decorrelation**
between the relative azimuthal angle jets, incompatible with $p\bar{p}$ Tevatron collider data
- a collinear treatment at next-to-leading order (NLO) can describe the data
- important issue: non-conservation of energy-momentum along the BFKL ladder. A LL BFKL-based Monte Carlo combined with e-m conservation improves dramatically the situation (Orr and Stirling)



Mueller Navelet jets at NLL BFKL

- up to now, the subseries $\alpha_s \sum (\alpha_s \ln s)^n$ NLL was included only in the exchanged Pomeron state, and not inside the jet vertices
Sabio Vera, Schwennsen
Marquet, Royon
- the common belief was that these corrections should not be important



Angular coefficients

$$\mathcal{C}_m \equiv \int d\phi_{J1} d\phi_{J2} \cos(m(\phi_{J1} - \phi_{J2} - \pi)) \\ \times \int d^2\mathbf{k}_1 d^2\mathbf{k}_2 \Phi(\mathbf{k}_{J1}, x_{J1}, -\mathbf{k}_1) G(\mathbf{k}_1, \mathbf{k}_2, \hat{s}) \Phi(\mathbf{k}_{J2}, x_{J2}, \mathbf{k}_2).$$

- $m = 0 \implies$ cross-section

$$\frac{d\sigma}{d|\mathbf{k}_{J1}| d|\mathbf{k}_{J2}| dy_{J1} dy_{J2}} = \mathcal{C}_0$$

- $m > 0 \implies$ azimuthal decorrelation

$$\langle \cos(m\phi) \rangle \equiv \langle \cos(m(\phi_{J1} - \phi_{J2} - \pi)) \rangle = \frac{\mathcal{C}_m}{\mathcal{C}_0}$$

Rely on LL BFKL eigenfunctions

- LL BFKL eigenfunctions:

$$E_{n,\nu}(\mathbf{k}_1) = \frac{1}{\pi\sqrt{2}} (\mathbf{k}_1^2)^{i\nu - \frac{1}{2}} e^{in\phi_1}$$

- decompose Φ on this basis
- use the known LL eigenvalue of the BFKL equation on this basis:

$$\omega(n, \nu) = \bar{\alpha}_s \chi_0(|n|, \frac{1}{2} + i\nu)$$

$$\text{with } \chi_0(n, \gamma) = 2\Psi(1) - \Psi\left(\gamma + \frac{n}{2}\right) - \Psi\left(1 - \gamma + \frac{n}{2}\right)$$

$$(\Psi(x) = \Gamma'(x)/\Gamma(x), \bar{\alpha}_s = N_c \alpha_s / \pi)$$

- \implies master formula:

$$\mathcal{C}_m = (4 - 3\delta_{m,0}) \int d\nu C_{m,\nu}(|\mathbf{k}_{J1}|, x_{J1}) C_{m,\nu}^*(|\mathbf{k}_{J2}|, x_{J2}) \left(\frac{\hat{s}}{s_0}\right)^{\omega(m,\nu)}$$

$$\text{with } C_{m,\nu}(|\mathbf{k}_J|, x_J) = \int d\phi_J d^2\mathbf{k} dx f(x) V(\mathbf{k}, x) E_{m,\nu}(\mathbf{k}) \cos(m\phi_J)$$

- at NLL, same master formula: just change $\omega(m, \nu)$ and V (although $E_{n,\nu}$ are not anymore eigenfunctions)

NLL Green's function: rely on LL BFKL eigenfunctions

- NLL BFKL kernel is not conformal invariant
- LL $E_{n,\nu}$ are not anymore eigenfunction
- this can be overcome by considering the eigenvalue as an operator with a part containing $\frac{\partial}{\partial \nu}$
- it acts on the impact factor

$$\omega(n, \nu) = \bar{\alpha}_s \chi_0 \left(|n|, \frac{1}{2} + i\nu \right) + \bar{\alpha}_s^2 \left[\chi_1 \left(|n|, \frac{1}{2} + i\nu \right) - \frac{\pi b_0}{2N_c} \chi_0 \left(|n|, \frac{1}{2} + i\nu \right) \underbrace{\left\{ -2 \ln \mu_R^2 - i \frac{\partial}{\partial \nu} \ln \frac{C_{n,\nu}(|\mathbf{k}_{J1}|, x_{J,1})}{C_{n,\nu}(|\mathbf{k}_{J2}|, x_{J,2})} \right\}}_{2 \ln \frac{|\mathbf{k}_{J1}| \cdot |\mathbf{k}_{J2}|}{\mu_R^2}} \right],$$

Collinear improved Green's function at NLL

- one may improve the NLL **BFKL** kernel for $n = 0$ by imposing its compatibility with **DGLAP** in the collinear limit
Salam; Ciafaloni, Colferai
- usual (anti)collinear poles in $\gamma = 1/2 + i\nu$ (resp. $1 - \gamma$) are shifted by $\omega/2$
- one practical implementation:
 - the new kernel $\bar{\alpha}_s \chi^{(1)}(\gamma, \omega)$ with shifted poles replaces

$$\bar{\alpha}_s \chi_0(\gamma, 0) + \bar{\alpha}_s^2 \chi_1(\gamma, 0)$$

- $\omega(0, \nu)$ is obtained by solving the implicit equation

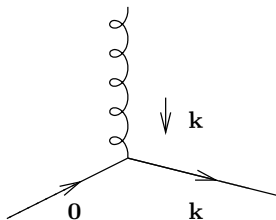
$$\omega(0, \nu) = \bar{\alpha}_s \chi^{(1)}(\gamma, \omega(0, \nu))$$

for $\omega(n, \nu)$ numerically.

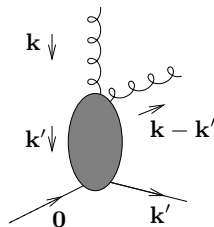
- there is no need for any jet vertex improvement because of the absence of γ and $1 - \gamma$ poles (numerical proof using **Cauchy** theorem "backward")

$\mathbf{k}, \mathbf{k}' =$ Euclidian two dimensional vectors

LL jet vertex:



NLL jet vertex:



$$V_a^{(0)}(\mathbf{k}, x) = h_a^{(0)}(\mathbf{k}) \mathcal{S}_J^{(2)}(\mathbf{k}; x)$$

$$\text{with: } h_a^{(0)}(\mathbf{k}) = \frac{\alpha_s}{\sqrt{2}} \frac{C_{A/F}}{\mathbf{k}^2},$$

$$\mathcal{S}_J^{(2)}(\mathbf{k}; x) = \delta\left(1 - \frac{x_J}{x}\right) |\mathbf{k}_J| \delta^{(2)}(\mathbf{k} - \mathbf{k}_J)$$

$$\begin{aligned}
 V_q^{(1)}(\mathbf{k}, x) = & \left[\left(\frac{3}{2} \ln \frac{\mathbf{k}^2}{\Lambda^2} - \frac{15}{4} \right) \frac{C_F}{\pi} + \left(\frac{85}{36} + \frac{\pi^2}{4} \right) \frac{C_A}{\pi} - \frac{5}{18} \frac{N_f}{\pi} - b_0 \ln \frac{\mathbf{k}^2}{\mu^2} \right] V_q^{(0)}(\mathbf{k}, x) \\
 & + \int dz \left(\frac{C_F}{\pi} \frac{1-z}{2} + \frac{C_A}{\pi} \frac{z}{2} \right) V_q^{(0)}(\mathbf{k}, xz) \\
 & + \frac{C_A}{\pi} \int \frac{d^2 \mathbf{k}'}{\pi} \int dz \left[\frac{1 + (1-z)^2}{2z} \left((1-z) \frac{(\mathbf{k} - \mathbf{k}') \cdot ((1-z)\mathbf{k} - \mathbf{k}')}{(\mathbf{k} - \mathbf{k}')^2 ((1-z)\mathbf{k} - \mathbf{k}')^2} h_q^{(0)}(\mathbf{k}') S_J^{(3)}(\mathbf{k}', \mathbf{k} - \mathbf{k}', xz; x) \right. \right. \\
 & \quad \left. \left. - \frac{1}{\mathbf{k}'^2} \Theta(\Lambda^2 - \mathbf{k}'^2) V_q^{(0)}(\mathbf{k}, xz) \right) \right. \\
 & \quad \left. - \frac{1}{z(\mathbf{k} - \mathbf{k}')^2} \Theta(|\mathbf{k} - \mathbf{k}'| - z(|\mathbf{k} - \mathbf{k}'| + |\mathbf{k}'|)) V_q^{(0)}(\mathbf{k}', x) \right] \\
 & + \frac{C_F}{2\pi} \int dz \frac{1+z^2}{1-z} \int \frac{d^2 \mathbf{l}}{\pi \mathbf{l}^2} \left[\frac{\mathcal{N} C_F}{\mathbf{l}^2 + (1-\mathbf{k})^2} (S_J^{(3)}(z\mathbf{k} + (1-z)\mathbf{l}, (1-z)(\mathbf{k} - \mathbf{l}), x(1-z); x) \right. \\
 & \quad \left. + S_J^{(3)}(\mathbf{k} - (1-z)\mathbf{l}, (1-z)\mathbf{l}, x(1-z); x) \right. \\
 & \quad \left. - \Theta \left(\frac{\Lambda^2}{(1-z)^2} - \mathbf{l}^2 \right) \left(V_q^{(0)}(\mathbf{k}, x) + V_q^{(0)}(\mathbf{k}, xz) \right) \right] \\
 & - \frac{2C_F}{\pi} \int dz \left(\frac{1}{1-z} \right) \int \frac{d^2 \mathbf{l}}{\pi \mathbf{l}^2} \left[\frac{\mathcal{N} C_F}{\mathbf{l}^2 + (1-\mathbf{k})^2} S_J^{(2)}(\mathbf{k}, x) - \Theta \left(\frac{\Lambda^2}{(1-z)^2} - \mathbf{l}^2 \right) V_q^{(0)}(\mathbf{k}, x) \right]
 \end{aligned}$$

$$\begin{aligned}
 V_g^{(1)}(\mathbf{k}, x) = & \left[\left(\frac{11}{6} \frac{C_A}{\pi} - \frac{1}{3} \frac{N_f}{\pi} \right) \ln \frac{\mathbf{k}^2}{\Lambda^2} + \left(\frac{\pi^2}{4} - \frac{67}{36} \right) \frac{C_A}{\pi} + \frac{13}{36} \frac{N_f}{\pi} - b_0 \ln \frac{\mathbf{k}^2}{\mu^2} \right] V_g^{(0)}(\mathbf{k}, x) \\
 & + \int dz \frac{N_f}{\pi} \frac{C_F}{C_A} z(1-z) V_g^{(0)}(\mathbf{k}, xz) \\
 & + \frac{N_f}{\pi} \int \frac{d^2 \mathbf{k}'}{\pi} \int_0^1 dz P_{qg}(z) \left[\frac{h_q^{(0)}(\mathbf{k}')}{(\mathbf{k} - \mathbf{k}')^2 + \mathbf{k}'^2} S_J^{(3)}(\mathbf{k}', \mathbf{k} - \mathbf{k}', xz; x) - \frac{1}{\mathbf{k}'^2} \Theta(\Lambda^2 - \mathbf{k}'^2) V_q^{(0)}(\mathbf{k}, xz) \right] \\
 & + \frac{N_f}{2\pi} \int \frac{d^2 \mathbf{k}'}{\pi} \int_0^1 dz P_{qg}(z) \frac{\mathcal{N}CA}{((1-z)\mathbf{k} - \mathbf{k}')^2} \left[z(1-z) \frac{(\mathbf{k} - \mathbf{k}') \cdot \mathbf{k}'}{(\mathbf{k} - \mathbf{k}')^2 \mathbf{k}'^2} S_J^{(3)}(\mathbf{k}', \mathbf{k} - \mathbf{k}', xz; x) \right. \\
 & \quad \left. - \frac{1}{\mathbf{k}^2} \Theta(\Lambda^2 - ((1-z)\mathbf{k} - \mathbf{k}')^2) S_J^{(2)}(\mathbf{k}, x) \right] \\
 & + \frac{CA}{\pi} \int_0^1 \frac{dz}{1-z} [(1-z)P(1-z)] \int \frac{d^2 \mathbf{l}}{\pi \mathbf{l}^2} \left\{ \frac{\mathcal{N}CA}{\mathbf{l}^2 + (1-\mathbf{k})^2} [S_J^{(3)}(z\mathbf{k} + (1-z)\mathbf{l}, (1-z)(\mathbf{k} - \mathbf{l}), x(1-z); x) \right. \\
 & \quad \left. + S_J^{(3)}(\mathbf{k} - (1-z)\mathbf{l}, (1-z)\mathbf{l}, x(1-z); x)] \right. \\
 & \quad \left. - \Theta\left(\frac{\Lambda^2}{(1-z)^2} - \mathbf{l}^2\right) [V_g^{(0)}(\mathbf{k}, x) + V_g^{(0)}(\mathbf{k}, xz)] \right\} \\
 & - \frac{2CA}{\pi} \int_0^1 \frac{dz}{1-z} \int \frac{d^2 \mathbf{l}}{\pi \mathbf{l}^2} \left[\frac{\mathcal{N}CA}{\mathbf{l}^2 + (1-\mathbf{k})^2} S_J^{(2)}(\mathbf{k}, x) - \Theta\left(\frac{\Lambda^2}{(1-z)^2} - \mathbf{l}^2\right) V_g^{(0)}(\mathbf{k}, x) \right] \\
 & + \frac{CA}{\pi} \int \frac{d^2 \mathbf{k}'}{\pi} \int_0^1 dz \left[P(z) \left((1-z) \frac{(\mathbf{k} - \mathbf{k}') \cdot ((1-z)\mathbf{k} - \mathbf{k}')}{(\mathbf{k} - \mathbf{k}')^2 ((1-z)\mathbf{k} - \mathbf{k}')^2} h_g^{(0)}(\mathbf{k}') \right. \right. \\
 & \quad \left. \times S_J^{(3)}(\mathbf{k}', \mathbf{k} - \mathbf{k}', xz; x) - \frac{1}{\mathbf{k}'^2} \Theta(\Lambda^2 - \mathbf{k}'^2) V_g^{(0)}(\mathbf{k}, xz) \right) \\
 & \quad \left. - \frac{1}{z(\mathbf{k} - \mathbf{k}')^2} \Theta(|\mathbf{k} - \mathbf{k}'| - z(|\mathbf{k} - \mathbf{k}'| + |\mathbf{k}'|)) V_g^{(0)}(\mathbf{k}', x) \right]
 \end{aligned}$$

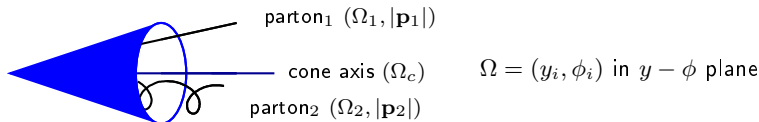
Jet algorithms

- a jet algorithm should be IR safe, both for soft and collinear singularities
- the most common jet algorithm are:
 - k_t algorithms (IR safe but time consuming for multiple jets configurations)
 - cone algorithm (not IR safe in general; can be made IR safe at NLO: Ellis, Kunszt, Soper)

Cone jet algorithm at NLO (Ellis, Kunszt, Soper)

- Should partons $(|\mathbf{p}_1|, \phi_1, y_1)$ and $(|\mathbf{p}_2|, \phi_2, y_2)$ be combined in a single jet?
 $|\mathbf{p}_i|$ = transverse energy deposit in the calorimeter cell i of parameter $\Omega = (y_i, \phi_i)$ in $y - \phi$ plane
- define transverse energy of the jet: $p_J = |\mathbf{p}_1| + |\mathbf{p}_2|$
- jet axis:

$$\Omega_c \begin{cases} y_J = \frac{|\mathbf{p}_1| y_1 + |\mathbf{p}_2| y_2}{p_J} \\ \phi_J = \frac{|\mathbf{p}_1| \phi_1 + |\mathbf{p}_2| \phi_2}{p_J} \end{cases}$$



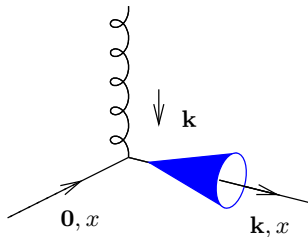
If distances $|\Omega_i - \Omega_c|^2 \equiv (y_i - y_c)^2 + (\phi_i - \phi_c)^2 < R^2$ ($i = 1$ and $i = 2$)

\Rightarrow partons 1 and 2 are in the same cone Ω_c

combined condition: $|\Omega_1 - \Omega_2| < \frac{|\mathbf{p}_1| + |\mathbf{p}_2|}{\max(|\mathbf{p}_1|, |\mathbf{p}_2|)} R$

LL jet vertex and cone algorithm

$\mathbf{k}, \mathbf{k}' =$ Euclidian two dimensional vectors

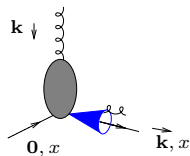


$$\mathcal{S}_J^{(2)}(k_{\perp}; x) = \delta\left(1 - \frac{x_J}{x}\right) |\mathbf{k}| \delta^{(2)}(\mathbf{k} - \mathbf{k}_J)$$

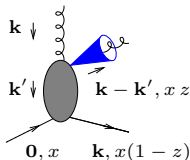
NLL jet vertex and cone algorithm

$\mathbf{k}, \mathbf{k}' =$ Euclidian two dimensional vectors

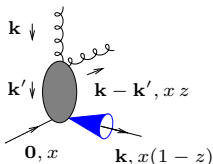
$$\mathcal{S}_J^{(3,\text{cone})}(\mathbf{k}', \mathbf{k} - \mathbf{k}', xz; x) =$$



$$\mathcal{S}_J^{(2)}(\mathbf{k}, x) \Theta \left(\left[\frac{|\mathbf{k} - \mathbf{k}'| + |\mathbf{k}'|}{\max(|\mathbf{k} - \mathbf{k}'|, |\mathbf{k}'|)} R_{\text{cone}} \right]^2 - [\Delta y^2 + \Delta \phi^2] \right)$$



$$+ \mathcal{S}_J^{(2)}(\mathbf{k} - \mathbf{k}', xz) \Theta \left([\Delta y^2 + \Delta \phi^2] - \left[\frac{|\mathbf{k} - \mathbf{k}'| + |\mathbf{k}'|}{\max(|\mathbf{k} - \mathbf{k}'|, |\mathbf{k}'|)} R_{\text{cone}} \right]^2 \right)$$



$$+ \mathcal{S}_J^{(2)}(\mathbf{k}', x(1-z)) \Theta \left([\Delta y^2 + \Delta \phi^2] - \left[\frac{|\mathbf{k} - \mathbf{k}'| + |\mathbf{k}'|}{\max(|\mathbf{k} - \mathbf{k}'|, |\mathbf{k}'|)} R_{\text{cone}} \right]^2 \right),$$

Using a IR safe jet algorithm, Mueller-Navelet jets at NLL are finite

- UV sector:

- the NLL impact factor contains UV divergencies $1/\epsilon$
- they are absorbed by the renormalization of the coupling: $\alpha_S \longrightarrow \alpha_S(\mu_R)$

- IR sector:

- PDF have IR collinear singularities: pole $1/\epsilon$ at LO
- these collinear singularities can be compensated by collinear singularities of the two jets vertices and the real part of the BFKL kernel
- the remaining collinear singularities compensate exactly among themselves
- soft singularities of the real and virtual BFKL kernel, and of the jets vertices compensates among themselves

This was shown for both quark and gluon initiated vertices (Bartels, Colferai, Vacca)

- one sums up $\sum (\alpha_s \ln \hat{s}/s_0)^n + \alpha_s \sum (\alpha_s \ln \hat{s}/s_0)^n$ ($\hat{s} = x_1 x_2 s$)
- at LL s_0 is arbitrary
- natural choice: $s_0 = \sqrt{s_{0,1} s_{0,2}}$ $s_{0,i}$ for each of the scattering objects
 - possible choice: $s_{0,i} = (|\mathbf{k}_J| + |\mathbf{k}_J - \mathbf{k}|)^2$ (Bartels, Colferai, Vacca)
 - but depend on \mathbf{k} , which is integrated over
 - \hat{s} is not an external scale ($x_{1,2}$ are integrated over)
 - we prefer

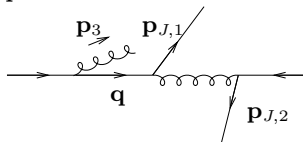
$$\left. \begin{aligned} s_{0,1} &= (|\mathbf{k}_{J1}| + |\mathbf{k}_{J1} - \mathbf{k}_1|)^2 \rightarrow s'_{0,1} = \frac{x_1^2}{x_{J,1}^2} \mathbf{k}_{J1}^2 \\ s_{0,2} &= (|\mathbf{k}_{J2}| + |\mathbf{k}_{J2} - \mathbf{k}_2|)^2 \rightarrow s'_{0,2} = \frac{x_2^2}{x_{J,2}^2} \mathbf{k}_{J2}^2 \end{aligned} \right\} \quad \frac{\hat{s}}{s_0} \rightarrow \frac{\hat{s}}{s'_0} = \frac{x_{J,1} x_{J,2} s}{|\mathbf{k}_{J1}| |\mathbf{k}_{J2}|} = e^{y_{J,1} - y_{J,2}} \equiv e^Y$$

- $s_0 \rightarrow s'_0$ affects
 - the BFKL NLL Green function
 - the impact factors:

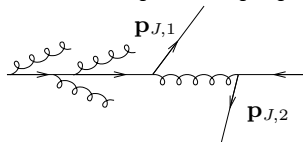
$$\Phi_{\text{NLL}}(\mathbf{k}_i; s'_{0,i}) = \Phi_{\text{NLL}}(\mathbf{k}_i; s_{0,i}) + \int d^2 \mathbf{k}' \Phi_{\text{LL}}(\mathbf{k}'_i) \mathcal{K}_{\text{LL}}(\mathbf{k}'_i, \mathbf{k}_i) \frac{1}{2} \ln \frac{s'_{0,i}}{s_{0,i}} \quad (1)$$

- numerical stability (non azimuthal averaging of LL subtraction) improved with the choice $s_{0,i} = (\mathbf{k}_i - 2\mathbf{k}_{Ji})^2$
(then replaced by $s'_{0,i}$ after numerical integration)
- (1) can be used to test $s_0 \rightarrow \lambda s_0$ dependence

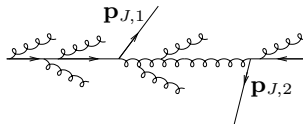
- Initial state radiation (unseen) produces divergencies if one touches the collinear singularity $q^2 \rightarrow 0$



- they are compensated by virtual corrections
- this compensation is in practice difficult to implement when for some reason this additional emission is in a "corner" of the phase space (dip in the differential cross-section)
- this is the case when $\mathbf{p}_1 + \mathbf{p}_2 \rightarrow 0$
- this calls for a resummation of large remaining logs \Rightarrow Sudakov resummation



- since these resummation have never been investigated in this context, one should better avoid that region
- note that for **BFKL**, due to additional emission between the two jets, one may expect a less severe problem (at least a smearing in the dip region $|\mathbf{p}_1| \sim |\mathbf{p}_2|$)



- this may however not mean that the region $|\mathbf{p}_1| \sim |\mathbf{p}_2|$ is perfectly trustable even in a **BFKL** type of treatment
- we now investigate a region where NLL **DGLAP** is under control